Wall-Jet along a Circular Cylinder in a Uniform Flow —its mixing region—

by

Fumio YOSHINO* and Ryoji WAKA*

(Received May 1, 1973)

There is presented the half of the investigation that had been carried out on the velocity distribution of the jet around and the aerodynamic force acting on a circular cylinder with tangential injection of air. It was found that separation bubble is formed at the point of discontinuity of the curvature of the wall and the differential equation of the thickness of jet can accurately predict the real thickness.

1 Introduction

It has been well known for a long time that the jet flows along the cylinder surface when it is injected to the tangential direction on the circular cylinder. This is the so-called Coanda effect. A number of investigations[1] were carried out under the condition that the air is injected but the main flow does not exist. There is only a few cases in which the velocity distribution of the flow is measured when the main flow exists, however. On the other hand, making use of the Coanda effect, we can control the boundary layer and obtain the high lift on a circular cylinder.

Dunham[2] and others carried out an investigation on this subject. But, we can hardly find the detailed investigation in which the position of the slot is extensively varied at a small value of C_μ. In this report, we carried out the experiment more systematically to get the velocity distribution in the mixing region of the flow when the position of the slot and the strength of the injection are varied at rather small Reynolds Number, while two dimensionality of the flow being carefully kept.

2 Nomenclature

R & B : Radius and span of the circular cylinder

s : Width of the slot

z : Distance from the center of the span in the spanwise direction (starbo-

* Department of Mechanical Engineering

ard is plus)

y : Distance from the wall in the radial direction

y_m & $y_{m/2}$: y at $u=u_m$ and $u=(u_m+U)/2$ respectively

b : Thickness of the mixing region of the jet

θ : Angle measured clockwise from the leading edge(Fig. 1 (a))

θ_J : Angle between the top of the cylinder and the slot (Fig. 1 (a))

φ : Angle measured clockwise from the slot $(= \theta - (\frac{\pi}{2} + \theta_J))$

ψ : $(= \frac{\pi}{180} \cdot \varphi)$

u : Velocity in the direction of θ at the point y

u_m : Maximum velocity in the cross-section of the jet

U : Velocity at the outer edge of the jet

m : Velocity ratio $(= U/u_m)$

P_∞ : Static pressure in the test section of the wind tunnel

P_s : Static pressure on the circular cylinder

P_w : Pressure of the compressed air inside the circular cylinder

C_μ : Momentum coefficient (*momentum of the jet at the slot exit*$\times s$)$/(\rho_\infty U_\infty^2 R)$

U_∞ : Wind tunnel velocity

R_{off} : Reynolds Number $(= \{ (P_w - P_\infty) Rs/\rho\nu^2 \}^{1/2})$

R_{on} : Reynolds Number $(= 2 U_\infty R/\nu)$

ν : Kinematic viscosity

3 Experimental

3-1 Experimental installment

Fig. 1 (a) shows the cross-section of the model cylinder used in the experiment. The small cylinder, 25mm in diameter, is inscribed to the large pipe of 100mm in diameter and this small pipe makes a part of the nozzle wall. The jet is injected along the circular cylinder from the slot. This slot has a constant width of 0.55 $^{+\ 0.03}_{-\ 0.02}$mm over the whole span. Stays are equally spaced at four points to keep the slot width constant.

The circular cylinder can be rotated circumferencially, so that the slot can be fixed at any position. The outside of the model cylinder is made into a mirror-like surface by chrome-plating. This modle cylinder has 100mm outer diameter, 404mm

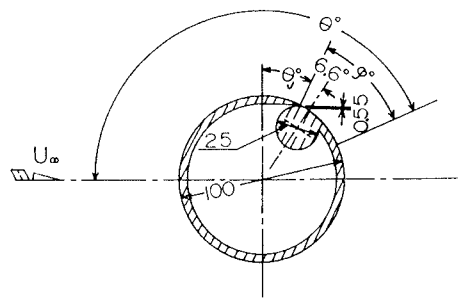

Fig. 1 (a) Cross-section of the circular cylinder.

spanwise width, and 35 static-pressure holes are made on the circumference at the center of the span. Inside of the model, 5 holes are arranged as equally as possible to measure the pressure inside of the cylinder.

Fig. 1 (b) shows the assembly drawing of the cylinder fixed on the three-component balance. The end plates with aerofoil section are installed at both ends of the cyliner. These dimensions are 62mm thick, 762 mm long and 362mm high.

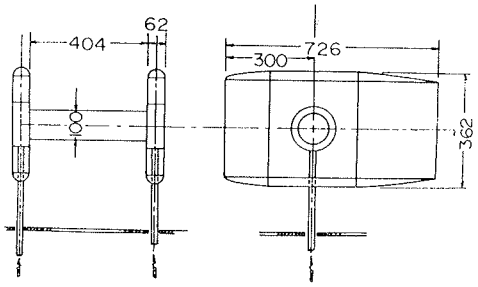

Fig. 1(b) Circular cylinder with end plates and struts.

The struts are connected with the cylinder inside the end plates and they are fixed on the three-component balance after passing through the bottom of the end plates and through the floor of the wind tunnel. The strut is hollow, so that the compressed air is supplied from both sides of the balance to the inside of the cylinder through flexible tubes made of cloth, through a stop valve and then through the inside of the strut.

The wind tunnel[3] used for the experiment is Goettingen type. The test section of the wind tunnel has the cross-section of 1.0×0.7m and its length is 1.5m. The maximum tunnel speed is measured about 52m/s and the ratio of the nozzle contraction is 6.

In order to measure the velocity distribution, a total head pitot tube was made by forming the cross-section of the tip of wire for a hypodermic needle into rectangle. This pitot tube is fixed on the micrometer and then this micrometer is attached to the circular-arc holding plate with the aerofoil section.

3-2 Experimental method

We carried out two kinds of measurement to check the velocity distribution. One is the case of injecting the jet only (with wind off) without the main flow and the other is the case of having both of the jet and the main flow. We measured the velocity distribution at many points along the flow direction mainly in the center section of the span. At the same time, we took measurements at several points in the spanwise direction to check the two dimensionality of jet.

In case of jet only, the slot position is fixed at $\theta_J = 0°$, and the measurement was carried out as in the following three cases; Reynolds Number $R_{off} = 1.61\times10^4$, 3.49×10^4 and 8.11×10^4. In this case, the atomospheric pressure is used as the reference static pressure to calculate velocity. We also took three sorts of measurements when the main flow exists. Here, the slot position is fixed at $\theta_J = 0°$ and C_μ is 0.085, 0.313 and 0.544, Reynolds Number $R_{on} = 3.2 \times 10^5$. We used the static pre-

ssure of the wall obtained in the center section as the reference static pressure to get the velocity. We corrected the error due to compressibility by the calculation[4] when velocity is high.

4 Results

4-1 The case without the main flow

Fig. 2 shows the velocity distribution at various points in both spanwise and flow directions, when $R_{off} = 3.49\times10^4$. In this case, it is seen that the flow is approximately two dimensional in full length of the span, excluding distortion of the velocity distribution near the outer edge of the profile at the position of $2Z/B = 0.594$ and $\varphi = 26.6°$.

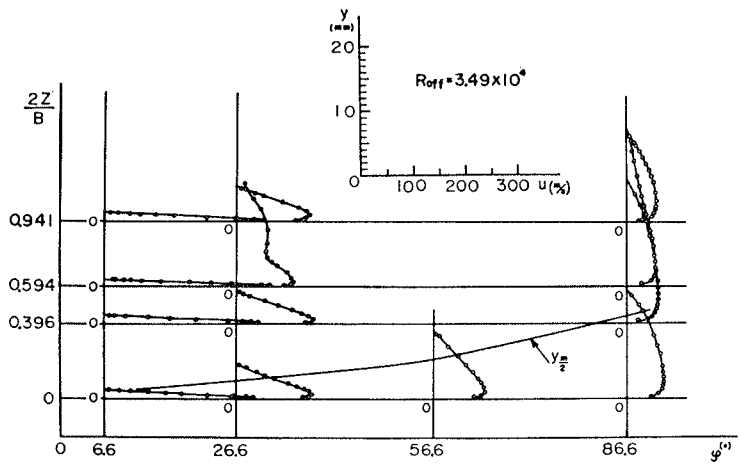

Fig. 2 Velocity distribution at various positions without main flow.

Fig. 3 (a) shows the velocity distribution of the mixing region of jet at four spanwise sections at $\varphi = 6.6°$. Fig. 3 (b) shows the velocity distribution at the same spanwise sections, but at $\varphi = 86.6°$. It is obvious that the velocity profile is similar in the spanwise direction when the position in the flow direction is same.

Tables I and II show the following ratios y_m/y_{mc}, $y_{\frac{m}{2}}/y_{\frac{m}{2}c}$ and u_m/u_{mc} at the three points of the flow direction, where y_m is the thickness of the boundary layer, $y_{\frac{m}{2}}$ thickness of the jet and u_m maximum velocity in the velocity profile. y_{mc}, $y_{\frac{m}{2}c}$ and

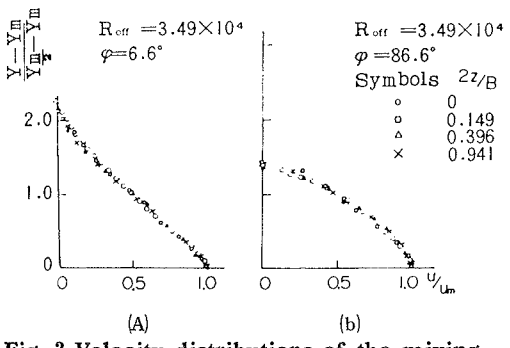

Fig. 3 Velocity distributions of the mixing region at various positions without main flow.

Table. I The values of y_m/y_{mc} $\left(y_{\frac{m}{2}}/y_{\frac{m}{2}c}\right)$, $R_{off}=3.49\times10^4$

φ° \ 2z/B	0	0.396	0.594	0.941
6.6	1.00 (1.00)	0.93 (0.93)	0.93 (0.93)	1.07 (1.16)
26.6	1.00 (1.00)	1.13 (1.10)	1.21 (3.59)	1.80 (1.20)
86.6	1.00 (1.00)	1.72 (1.37)	0.88 (1.17)	1.04 (0.84)

Table. II The values of u_m/u_{mc}, $R_{off}=3.49\times10^4$

φ° \ 2z/B	0	0.396	0.594	0.941
6.6	1.00	1.12	1.03	0.98
26.6	1.00	1.01	0.75	1.08
86.6	1.00	0.87	0.81	0.85

u_{mc} are the values in the center section.

From these tables, it comes out that the relative discrepancy to each other of the boundary layer thickness, jet thickness and the maximum velocity in the section is small in comparison with the span width, excluding the distortion of the above mentioned velocity distribution. Therefore, taking Fig. 3 into consideration, the jet is nealy two dimensional. The above mentioned fact is noticed in case of two other R_{off}s as well.

Fig. 4 shows the velocity distribution at various points in the flow direction at the center section of the span. This figure shows that the velocity at larger y is smaller than the velocity at other points, as far as the velocity distribution at $\varphi=86.6°$ is concerned.

Considering that we measured the very slow motion by a pitot tube, the error is to be great there.

From these facts, it is clear that the velocity distribution of the jet in our experiment is similar through the flow direction. The figure shows that the ratio of $y_m/y_{\frac{m}{2}}$ is almost constant, 0.2 in the flow direction.

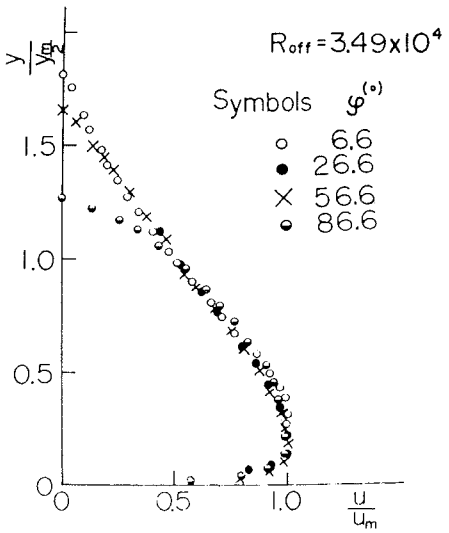

Fig. 4 Velocity distributions in the flow direction without main flow.

Then Fig. 5 shows the static pressure distribution on the wall in the flow direction. The full line in the figure is the experimental curve by Newman[5]. Our pressure coefficient approaches 0 earlier than Newman's. The figure indicates that our separation point is located near $\varphi_{sep}=190°$, and Newman's is backward by about 30°.

Fig. 6 shows the experimental ratio $y_{\frac{m}{2}}/R\psi$ to $y_{\frac{m}{2}}/R$. The relation at $y_{\frac{m}{2}}/R > 0.08$ ($\varphi > 26.6°$) is shown linear and it is expressed as follows;

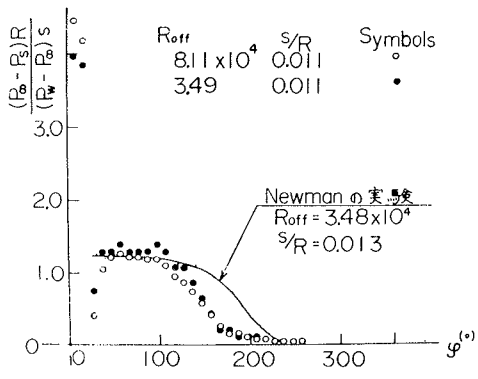

Fig. 5 Static-pressure distributions at the central section of the span without main flow.

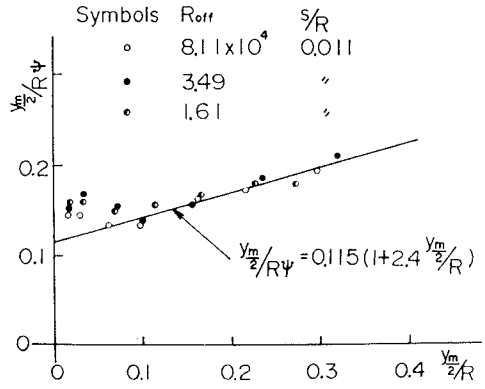

Fig. 6 Growth of the jet in flow direction.

$$\frac{y_{\frac{m}{2}}}{R\psi} = c\left(1 + k\frac{y_{\frac{m}{2}}}{R}\right) \tag{1}$$

where c = 0.115 and k = 2.4. These are a little larger than Newman's values c = 0.11 and k = 1.5.

4-2 The case with the main flow

To determine parameter C_μ, we used the jet velocity at the slot exit calculated from the air pressure and temperature inside the cylinder. Fig. 7 shows the velocity distributions at various sections and points in the flow direction when C_μ = 0.313. This figure shows clearly that the velocity reduces earlier very near the end plates than at other sections. This kind of things did not occur without the main

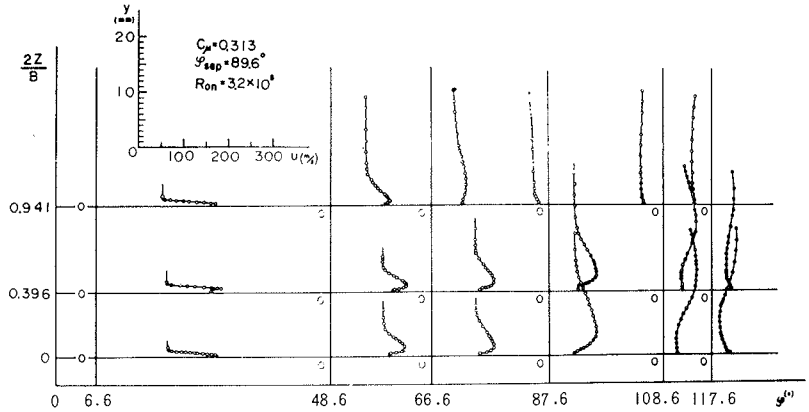

Fig. 7 Velocity distributions at various positions with main flow.

flow. On the other hand, the velocity distribution is approximately two dimensional near the center section of the span. But three dimensionality seems to appear near the separation point.

Fig. 8 is the velocity distribution in the mixing region at various sections in the spanwise direction where $C_\mu = 0.085$, $\varphi = 24.6°$ and $C_\mu = 0.544$ and $\varphi = 78.6°$. Very near the end plates, the velocity distribution shows that the velocity tends to get a little bigger at larger y than at other span sections. But this tendency is very small and the velocity distribution in the mixing region is approximately similar almost all over the span.

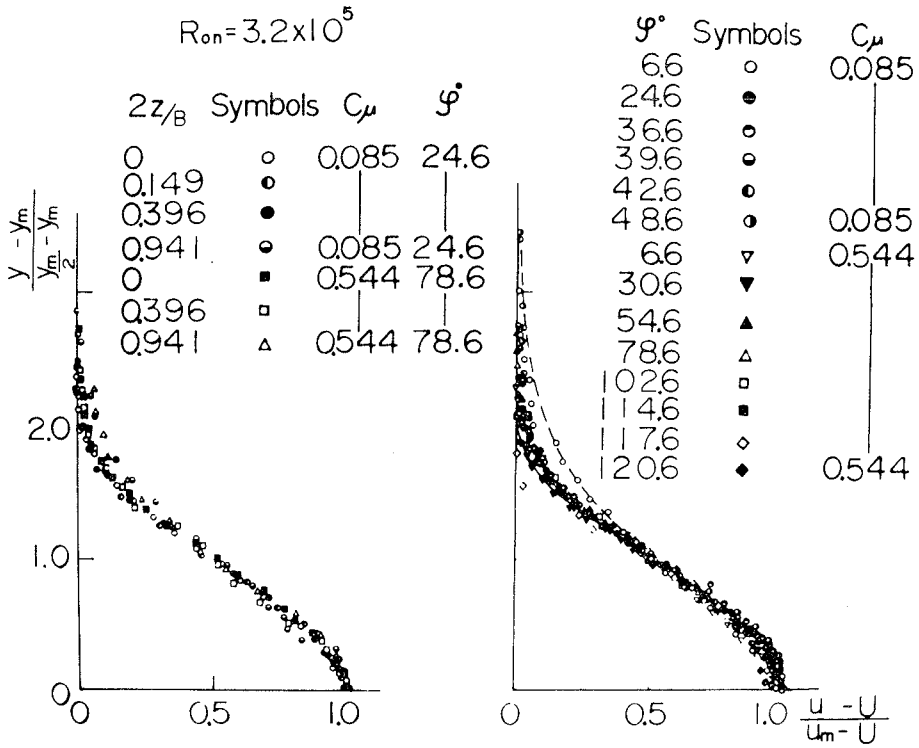

Fig. 8 Fig. 9 Velocity distributions of the mixing region at various sections (Fig. 8) and at various points in flow direction (Fig. 9).

Tables III and IV correspond respectively to Tables I and II which are for the case without the main flow. In this case, $C_\mu = 0.313$ and the separation point in the center section is $\varphi_{sep} = 89.6°$. Table IV indicates that the velocity reduces rapidly near the end plates, and the adverse flow is obviously seen at a smaller φ there than at the center section of the span.

Table III shows y_m and $y_{\frac{m}{2}}$ thicken early near the end plates. This corresponds to the result of Table IV. Excluding the flow near the separation point, however, the ratios of y_m/y_{mc}, $y_{\frac{m}{2}}/y_{\frac{m}{2}c}$ and u_m/u_{mc} are approximately 1.0 near the center

φ(°) \ z/B	-0.149	0	0.396	0.941
6.6	0.846 (0.920)	1.000 (1.000)	2.387 (1.330)	1.103 (0.946)
24.6	0.897 (0.976)	1.000 (1.000)	0.975 (1.001)	1.885 (1.363)
48.6	0.805 (0.905)	1.000 (1.000)	0.807 (0.842)	0.528 (0.907)
66.6	1.397 (1.164)	1.000 (1.000)	1.040 (0.969)	2.184 (2.037)
87.6	2.924 (1.511)	1.000 (1.000)	0.764 (0.737)	
108.6		1.000 (1.000)	0.831 (0.963)	

Table. Ⅲ The values of $y_m/3y_{mc}\left(y_{\frac{m}{2}}/\ y_{\frac{m}{2}c}\right)$, $C_\mu = 0.085$ **and** $R_{on}=.2\times10^5$.

φ(°) \ z/B	-0.149	0	0.396	0.941
6.6	1.011	1.000	1.051	1.046
24.6	1.008	1.000	1.025	1.021
48.6	0.979	1.000	1.035	0.856
66.6	0.957	1.000	1.021	0.625
87.6	0.681	1.000	1.022	-0.327
108.6		1.000	1.012	-0.534

Table. Ⅳ The values of u_m/u_{mc}, $C_\mu = 0.085$ **and** $R_{on} = 3.2\times10^5$.

section of the span. Taking the result of Fig. 8 into account, it can be said the flow near the center section of the span is almost two dimensional. But very near the separation point and the end plates, the flow is three dimensional. This is the point different from the case of the jet without the main flow.

Fig. 9 shows the velocity distribution of the mixing region at the center section of the span. This distribution is measured at various positions in the flow direction. The figure shows two cases where $C_\mu = 0.085$ and 0.544. From this figure, we find the velocity distribution in the mixing region is similar irrespective of the value of C_μ and the position of the flow direction. The fact that the separation point of $\varphi_{sep} = 96.6°$, when $C_\mu = 0.544$, shows that the velocity distribution keeps similarity even after passing the separation point.

The broken line in the figure shows the hyperbolic function expressed by

$$\frac{u-U}{u_m-U} = sech^2\left\{0.88\times\frac{y-y_m}{y_{\frac{m}{2}}-y_m}\right\} \tag{2}$$

The full line shows the cosine function;

$$\frac{u-U}{u_m-U} = \frac{1}{2}\left\{1-\cos\pi\frac{y-y_m}{b}\right\} \tag{3}$$

The full line has a good agreement with the experiment compared with the broken line, although this cosine curve slightly underestimates the velocity at larger y. That is, the velocity distribution in the mixing region can be expressed by the equation (3), when there is the main flow.

Figs. 10(a) and (b) respectively show variation of y_m/R, $y_{\frac{m}{2}}/R$ and m in the flow

direction at the center section of the span. From Fig. 10, it is known that the thickness of the jet $y_{\frac{m}{2}}/R$ increases correspondingly to the increase of the thickness of the boundary layer. Fig. 10 shows, in this case, that the value of m does not become 1 until it reaches the separation point, and after separation, it approaches 1 rapidly.

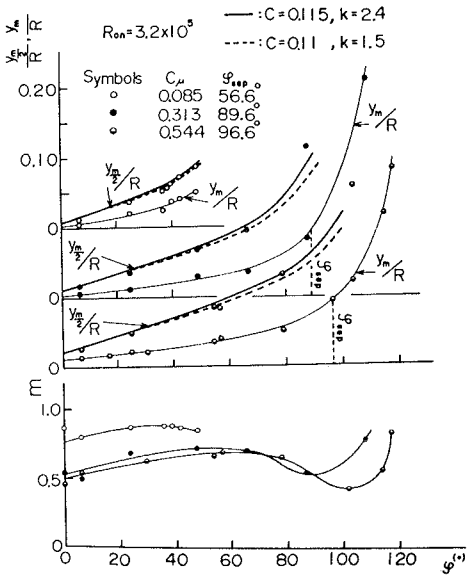

Fig. 10 variations of y_m/R and $y_{\frac{m}{2}}/R$ (a) and m (b) in the flow direction.

5 Discussion

5-1 The case without the main flow

As we mentioned before, in this experiment the ratio of the thickness of jet to the thickness of the boundary layer, $y_m/y_{\frac{m}{2}}$ is about 0.2 and this is larger than the value of Newman's experiment 0.14. In our experiment, the separation point is φ_{sep} = 190°, but Newman's is a about 220°. Furthermore, the constants in the equation (1), c and k are a little bit larger than Newman's. These mean that the jet thickness in our experiment grows relatively rapidly. According to Newman, $y_m/y_{\frac{m}{2}}$, c and k become larger when Reynolds Number, R_{off}, gets smaller than 4×10^4 and the separation point moves forward. As shown in Fig. 5, Reynolds Number of the experiment is nearly same, so we do not consider that the value of R_{off} caused to thicken the jet thickness. On the other hand, according to Fernholz[6], when the ratio of the slot width to the cylinder radius s/R is within the limit of $0.053 \geqq s/R \geqq 0.0074$, the separation point of the flow is same as far as compared by the same value of R_{off} and the velocity distribution of the part of boundary layer, in case of turbulent flow forms the Glauert[7]'s turbulent velocity distribution of the wall jet along the plate. It seems to be unreasonable to attribute it to the slot width, because of s/R = 0.011 in our experiment. Assuming that the jet injected from the slot is an inviscid fluid and it flows along the wall keeping its thickness equal to the slot width, we can have the following equation (4)[6], if it is incompressible fluid,

$$\frac{P_\infty - P_s}{P_w - P_\infty} = 2\frac{s}{R} + \left(\frac{s}{R}\right)^2 \tag{4}$$

In this experiment, the jet injected from the slot flows first along the small cylinder with the diameter of 25mm, and second it flows along the larger cylinder with the diameter of 100mm after passing the contact point of the small cylinder with the main cylinder. s/R varies discontinuously from 0.044 to 0.011 before and after this contact point. In such the flow, the static pressure rises discontinuously from 0.09 to 0.022 before and after the contact point. Or the ratio of $(P_\infty - P_s)\,R/(P_w - P_\infty)\,s$ goes up discontinuously from 8.2 to 2 before and after the contact point, where $R=50$mm. But the above assumption does not come into existence in the real flow. Therefore, the pressure rise will not occur so rapidly.

From Fig. 5, the static pressure between the contact point of the cylinders (φ = 6.6°) and 10° down stream is nearly constant and the value is about 4. The rapid rise of the pressure takes place between 10° and 20°, and then at 20° the pressure becomes around 0.5. After that, the pressure goes down to about 1.25 and remains at this value. For about 10 degrees after the contact point, pressure is kept relatively low. This resembles the pressure of the separation bubble near the leading edge of the aerofoil, so it appears to be the separation of laminar flow but it can be turbulent flow since the value of $y_m\sqrt{u_m/\nu}$ [8] is larger than 9 near the contact point. We can only consider discontinuity of the radius of curvature makes boundary layer thicker and its turbulence stronger. We may conclude that the turbulence of our jet is intensive, the ratio $y_m/y_{\frac{m}{2}}$ gets bigger, the thickness of the jet grows relatively rapidly and the separation point moves forward owing to this reason.

5-2 The case with the main flow

As mentioned before, the velocity distribution in the mixing region is similar until it passes the separation point in case with the main flow and the profile is approximated by the equation (3). This similarity is independent of C_μ as far as this experiment goes.

When the velocity distribution is similar, the jet thickness is the function of the central angle ψ which is measured from the slot and the velocity ratio m ($= U/u_m$). Then the following equation[9] is derived,

$$\frac{dy_{\frac{m}{2}}}{d\psi} = \frac{1+m}{1-ck\psi+m(1+ck\psi)}\frac{dy_m}{d\psi} + \frac{c(1-m)}{1-ck\psi+m(1+ck\psi)}(R+k\,y_{\frac{m}{2}}) \tag{5}$$

In the above equation, c and k are identical with c and k of the equation (1) and m = 0.5 when $m \geqq 0.5$.

To check if the above equation holds or not, we numerically integrated the equa-

tion (5) making use of a computer, where the experimental value of y_m (Fig. 10 (a)) and $m = 0.5$ were used. In Fig. 10 (b), up until the separation point $m \geqq 0.5$ so that $m = 0.5$, the initial value of $y_{\frac{m}{2}}$ is taken as the value at the intersection of the extension of the curve which smoothly connects the experimental points (Fig. 10 (a)) with the straight line $\varphi = 0°$. The thick full line in Fig. 10 (a) shows the result of the calculation in which we used the constants $c = 0.115$, and $k = 2.4$ (Fig. 6) of our jet and the broken line is the case by the constants of Newman and others, that is $c = 0.11$ and $k = 1.5$.

As the figure shows clearly, the value obtained by calculation seems to be within the experimental error near the slot with either constants. The closer it gets to the separation point, however, the better the value calculated with our values of $c = 0.115$ and $k = 2.4$ agrees with the experimental value.

We already discussed why our c and k are different from those of Newman's. When there is the main flow, the influence of the following factors should be taken into account: the boundary layer thickness of the main flow upstream of the slot, the shape and thickness of the upper lip. But we consider these effects can be ignored due to the next reasons. That is, the influence of the boundary layer thickness seems not to be dependent on models, since the boundary layer thickness of the upstream is determined by Reynolds Number only if the wall is hydrodynamically smooth. The influence of the upper-lip thickness of the slot can not be discussed directly, becanse there do not seem to exist other measurements of the velocity profile of jet with the main flow around a circular cylinder. According to the experiments[10)11)] on the effectiveness of film cooling over the flat plate, when $m \fallingdotseq 1$ and the thickness of the upper lip is thick compared with the slot width, the wake of the upper lip gets larger, the turbulence stronger, and then the effectiveness is reduced. When $m > 1$, the jet is pulled away off the wall to the main flow and the separation bubble appears right after the slot exit[12)]. The effectiveness approaches a certain constant, however, when the upper-lip thickness is thin enough in comparison with the slot width s and its ratio is smaller than 0.38. When $m \leqq 1$, the separation bubble disappears[10)].

This seems qualitatively true about the jet around the circular cylinder, too. So, the influence of the upper lip of the slot on the turbulence of the jet seems able to be ignored, if the upper lip of the slot is thin enough and $m \leqq 1$. In our case, the ratio of the upper-lip thickness to the slot width is about 0.2 and the upper lip is thinned to the tip so that the influence of the upper lip can be ignored. The wake of the upper lip is not seen in Fig. 7 even at right after the slot. This also true for the other values of C_μ.

From the facts mentioned above, it may be concluded that the curvature of the wall varied discontinuously at right after the slot results in that the values of c and k in case of the jet with the main flow are greater than those given by New-

man. This, in turn, means that $y_{\frac{m}{2}}$ can be calculated from the equation (5) by using the values for c and k given by Newman, if the jet is injected tangentially to the circular cylinder which has a constant curvature and the upper lip of the slot is thin enough.

The structure of the slot used by Newman, however, can not give us a good circularity. Therefore, it is more convenient to make use of the structure of our slot than Newman's in order to analyze the over-all flow around the cylinder, since our slot guarantees the good circularity. Of course, it must be kept in mind that the values of 0.115 and 2.4 for c and k respectively are used in the equation (5) when the slot is designed based on ours.

6 Conclusion

(1) The case without the main flow.
  (I) There exists a large negative pressure right after the slot exit. This takes place due to discontinuous increase of the radius of curvature of the wall where the jet flows along.
  (II) Therhfore, the jet thickness grows a little earlier than Newmsn's experiment.

(2) The case with the main flow.
  (I) A large negative pressure exists right after the slot exit due to the same reason as the case without the main flow. This is a local phenomenon, however.
  (II) The velocity distribution in the mixing region is similar as expressed by the equation (3). And it is still similar after passing the separation point.
  (III) Differential equation (5) is made sure to hold.

References

(1) Wille, R and Fernholz, J., J. Fluid Mech., **23**-4 (1965), 801.
(2) Dunham, J., Aeron. J., **74**(1970-1), 91.
(3) Yoshino and the other, Reports of the Faculty of Eng. Tottori Univ., **1**-1 (Showa 45-12), 7.
(4) Poff, Method of Aerodynamic Experiment in Mechanical Engineering, (Showa 44), 136, Asakura.
(5) Lachmann, G. V. (ed.), Boundary Layer and Flow Control, **1**, (1961), 232, Pergamon.
(6) Fernholz, H., Jahrbuch 1964 der WGLR, 149.
(7) Glauert, M. B., J. Fluid Mech., (1956), 625.
(8) Schlichting, H., Boundary Layer Theory, (1960), 36, McGraw-Hill.
(9) Yoshino and Furuya, Preprint of Bulletin of JSME, No.723-2 (Showa47-3), 121.
(10) Kacker, S. C. and Whitelaw, J. H., Trans. ASME, Ser. C, **90**-4 (1968-11), 469.
(11) Kacker, S. C. and Whitelaw, J. H., Int. J. Heat & Mass Transf., **12** (1969-9), 1196.

(12) Burns, W. K. and Stollery, J. L., Int. J. Heat & Mass Transf., **12** (1969-11), 935.

(13) Yoshino and Waka, Reports of the Faculty of Eng. Tottori Univ., **3**-2 (1973-3), 25.